SCIENTIFIC REPORTS

OPEN

SUBJECT AREAS:
BATTERIES
POROUS MATERIALS

Received
28 August 2013

Accepted
13 January 2014

Published
3 February 2014

Correspondence and requests for materials should be addressed to G.L.C. (cuigl@qibebt.ac.cn)

Sustainable, heat-resistant and flame-retardant cellulose-based composite separator for high-performance lithium ion battery

Jianjun Zhang[1], Liping Yue[1,3], Qingshan Kong[1], Zhihong Liu[1], Xinhong Zhou[3], Chuanjian Zhang[1], Quan Xu[1], Bo Zhang[1], Guoliang Ding[1], Bingsheng Qin[1], Yulong Duan[1], Qingfu Wang[1], Jianhua Yao[1], Guanglei Cui[1] & Liquan Chen[2]

[1]Qingdao Key Lab of Solar Energy Utilization and Energy Storage Technology, Qingdao Institute of Bioenergy and Bioprocess Technology, Chinese Academy of Sciences, Qingdao 266101, P. R. China, [2]Beijing National Laboratory for Condensed Matter Physics, Institute of Physics, Chinese Academy of Sciences, Beijing 100190, P. R. China, [3]College of Chemistry and Molecular Engineering, Qingdao University of Science and Technology, Qingdao 266042, P. R. China.

A sustainable, heat-resistant and flame-retardant cellulose-based composite nonwoven has been successfully fabricated and explored its potential application for promising separator of high-performance lithium ion battery. It was demonstrated that this flame-retardant cellulose-based composite separator possessed good flame retardancy, superior heat tolerance and proper mechanical strength. As compared to the commercialized polypropylene (PP) separator, such composite separator presented improved electrolyte uptake, better interface stability and enhanced ionic conductivity. In addition, the lithium cobalt oxide ($LiCoO_2$)/graphite cell using this composite separator exhibited better rate capability and cycling retention than that for PP separator owing to its facile ion transport and excellent interfacial compatibility. Furthermore, the lithium iron phosphate ($LiFePO_4$)/lithium cell with such composite separator delivered stable cycling performance and thermal dimensional stability even at an elevated temperature of 120°C. All these fascinating characteristics would boost the application of this composite separator for high-performance lithium ion battery.

Lithium ion battery (LIB) has received wide-spread attention for large-scale power sources and promising energy storage devices owing to its high power, high energy density and long cyclelife[1–14]. Accordingly, there are increasing requirements for LIB key materials especially separator. LIB separator performed the crucial functions of physically separating the anode and cathode while permitting free flow of lithium ions[15–17]. It is well recognized that the microporous structure and thermal dimensional stability of separators considerably affect the battery performance, including power densities, cycle life and safety characteristics. Currently, polyolefin microporous membranes were the most widely used separators for commercial LIB due to their advantages, such as good electrochemical stability, proper thickness, and considerable mechanical strength[18,19]. Nevertheless, there is still quite challenging because polyolefin separators often suffer from poor electrolyte wettability and severe dimensional instability at an elevated operating temperature when the battery was running at high charge/discharge current[20,21]. Poor electrolyte wettability would lower rate capability of the battery because of high internal ionic resistance. In addition, severe dimensional instability may cause internal short-circuiting or lead to thermal runaway especially for use in batteries at high charge/discharge current. Therefore, it is mandatory to develop highly safe separators with good electrolyte wettability, superior thermal resistance and flame retardancy to improve the abuse tolerance of LIB.

From a practical point of view, an ideal separator should possess low cost, high electrolyte uptake, high thermal stability, excellent flame retardancy, proper mechanical strength and superior battery performance. Moreover, with exhausted fossil oil and severe environmental pollution, renewable polymers are highly motivated as an alternative to polyolefin-based materials[22]. It is well known that cellulose is one of the most abundant, renewable resources on the earth and possesses outstanding properties such as high dielectric constant, good chemical stability and superior thermal stability[23–26]. These excellent properties could qualify cellulose an ideal substitute

fossil-based separators for battery application. In recent years, many efforts have been made to develop high-performance separators from low cost, renewable cellulose[27–30]. It was reported that eco-friendly cellulose nanofibers can be successfully explored as a separator for LIB[28]. Cui et al. explored renewable, low cost and environmentally benign cellulose/poly (vinylidene fluoride-co-hexafluoropropylene) composite nonwoven as an advanced separator for high-performance LIB via an electrospinning technique followed by a dip-coating process[29]. Furthermore, the porous structure-tuned cellulose nanofiber separators were also developed as a promising alternative to commercial polyolefin separators for LIB via a facile fabrication strategy based on colloidal SiO_2 nanoparticle-assisted structural control by Lee and his coworker[30]. However, cellulose is highly flammable, which is unfavorable for safety concern when LIB was abused[31,32]. In terms of safety issue of LIB, it is critical to develop thermal resistant and flame-retardant cellulose separator.

Herein, we presented a renewable, flame-retardant and thermal resistant cellulose-based composite nonwoven separator (hereinafter, abbreviated as "FCCN separator") as LIB separator. To the best of our knowledge, this is the first scientific report that addresses highly flame-retardant FCCN separator of high-power LIB. Our results demonstrate that FCCN separator is a very promising separator to significantly improve the safety issue of LIB owing to its good flame retardancy, superior thermal stability and electrochemical characteristics. Another motivation of this work shed light on an ideal substituent of synthetic polymer derived from fossil oil by renewable polymer as clean energy material owing to its versatile diversity and easy processability.

Results

Preparation of FCCN separator. Figure 1 outlined the preparation process of the FCCN separator. Cellulose pulp (20 g), sodium alginate (SA) (10 g), flame retardant (FR) (10 g) and silica (5 g) were placed into 1 L deionized water and pulped for 5 h to yield completely dispersed FCCN suspension. The obtained FCCN suspension was poured on a papermaking machine followed by vacuum filtration to generate a wet FCCN paper. Then the wet FCCN paper was transferred to a plate dryer to remove additional water and subsequently rolled under a pressure of 10 MPa at 95°C, leading to the generation of a FCCN separator. Cellulose nonwoven separator without flame retardant, sodium alginate and silica (abbreviated as "CN separator") was prepared by papermaking method for a fair comparison.

Morphological and physical characterization. Typical SEM images of PP separator, CN separator and FCCN separator were demonstrated in Figure 2. PP separator showed uniform and typically elliptic pores, which were formed via a uniaxially stretching technology as revealed in Figure 2a[9]. The long axis of the pore was 100–500 nm and the short axis of about 50 nm. It was obviously observed in Figure 2b that CN separator consisted of randomly arranged fibers with diameter size of 2 ± 0.2 μm and it possessed excessively large-sized pores (>4 μm). Because of large pore size, pristine CN separator generally suffered from internal short circuit ascribed to lithium dendrites during the charge–discharge process[28]. Compared with CN separator, FCCN separator (Figure 2c–d) presented distributed pores with diameters ranging from 100 nm to 200 nm, which was expected to play a critical role in preventing internal short-circuits, avoiding self-discharge and achieving uniform current density especially for batteries operating at high charge/discharge rates[29]. In addition, this tortuous structure was favourable to prevent the growth of lithium dendrites, which was advantageous to battery safety[33,34].

Physical and electrochemical parameters of PP separator and FCCN separator were listed in Table 1. It should be noted that Gurley value of FCCN separator was 45 s, which was much lower than that of PP separator (235 s). It was well known that lower Gurley value of FCCN separator was attributed to highly porous structure of the membrane, which was well consistent with the SEM analysis. The improvement in the microporous structure of the separator was further confirmed by the porosity. Obviously, the porosity of FCCN separator (70%) was fairly higher than that of PP separator (55%). Tortuosity was used to provide information regarding the transport of ions on the effect of pore blockage, which was calculated from the porosity and the ionic conductivity[35]. Table 1 compared tortuosity calculated of PP separator and FCCN separator. As is well known, $\tau > 1$ is good for dendrite resistance but can lead to higher separator resistance. Here the τ value of FCCN separator was observed to encompass lower tortuosity value compared to PP separator favoring the dendrite resistance as well as reducing the separator resistance reasonably[1]. High porosity can result in high electrolyte uptake, and consequently lead to high ionic conductivity

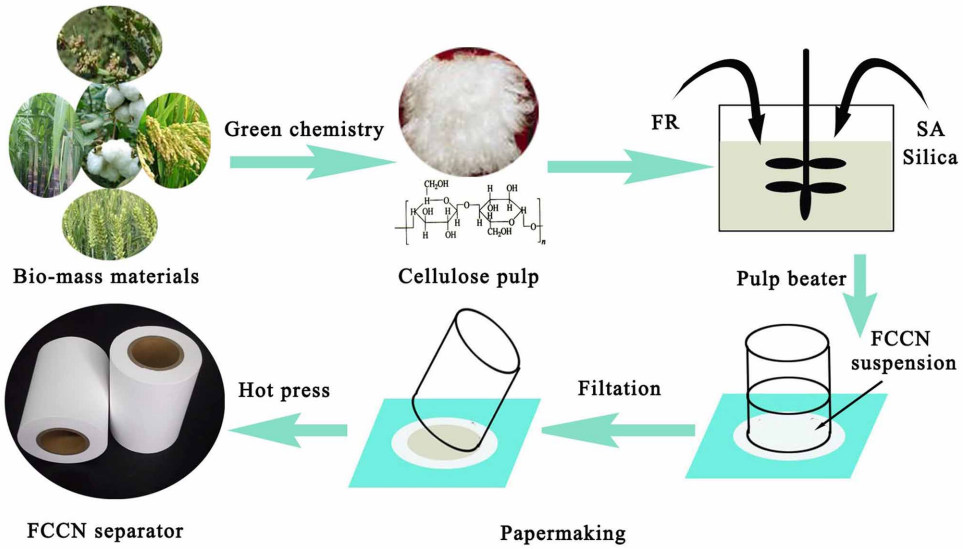

Figure 1 | Schematic illustration for the preparation process of FCCN separator. (We appreciated Chuanjian Zhang for his contribution in designing and drawing Figure 1).

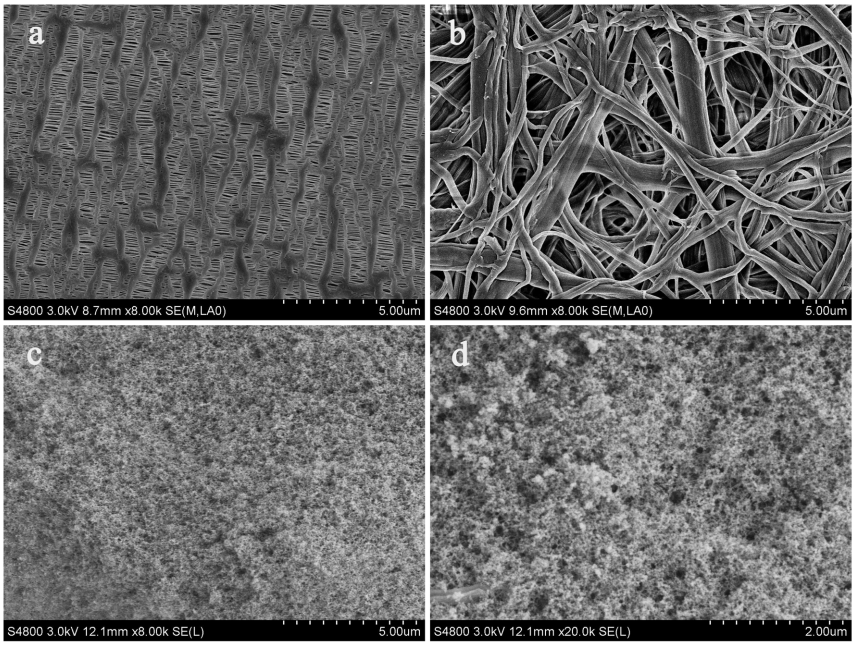

Figure 2 | Typical SEM micrographs of (a) PP separator (×8000), (b) CN separator (×8000), (c) FCCN separator (×8000) and (d) FCCN separator (×20000).

of electrolyte-soaked FCCN separator, which was favourable to facilitate rapid ionic transportation[36,37].

A separator should possess good electrolyte wettability to retain the electrolyte efficiently during the charge/discharge process[38]. Contact angle between the separators and liquid electrolyte (1 M $LiPF_6$ in EC/DMC) were conducted to characterize the electrolyte wettability of PP separator and FCCN separator. It was clearly displayed from Figure 3 that the contact angle of PP separator (84°) was much higher than that of FCCN separator (15°), which confirmed that FCCN separator exhibited better electrolyte wettability than PP separator[39]. The electrolyte wettability rate of PP separator and FCCN separator were also evaluated by comparing the electrolyte immersion-height of the separators (Figure S1). Obviously, the immersion-height of FCCN separator (2.9 cm) was greater than that of PP separator (0.2 cm). The higher immersion-height verified that FCCN separator was more lyophilic to liquid electrolyte. As a method for quantitative testing, the electrolyte uptake was listed in Table 1. The electrolyte uptake of FCCN separator was 270%, which was higher than that of PP separator (125%). This remarkable liquid electrolyte wettability of FCCN separator may be ascribed to the well interconnected microporous structure and the intrinsically lyophilic nature of cellulose material. Thus, high porosity, lower Gurley value, and superior electrolyte wettability of FCCN separator were beneficial to improve the rate capability and cycling stability of LIB[16].

Lithium ion battery separator should be enough mechanically robust to withstand the high tension after casual collisions and prevent internal short-circuits caused by the rough electrode surface, debris and growth of lithium dendrite[1,19]. The stress-strain curves of PP separator, CN separator and FCCN separator were depicted in Figure S2. It was clearly demonstrated that FCCN separator exhibited an enhanced tensile strength of 45 MPa and deformation of 6.5%, which was much higher than that of CN separator (22 MPa with deformation of 3.5%). Obviously, the tensile strength of FCCN separator was much better than the transverse strength of PP separator (12 MPa) and lower than that of PP separator at the machine direction (120 MPa)[40]. PP separator was prepared via a uniaxially stretching technology. Different orientations at vertical and horizontal directions lead to the different tensile strength. However, FCCN separator was fabricated by papermaking process. The distribution of cellulose microfibers in FCCN separator was uniform, thus, tensile strength is same at both vertical and horizontal directions. In addition, sodium alginate and silica nanoparticles were used for bonding cellulose fiber, further enhancing the tensile strength of FCCN separator. So, the tensile strength of FCCN separator was much better than the transverse strength of PP separator (12 MPa) and lower than that of PP separator at the machine direction (120 MPa). Interestingly, FCCN separator has a considerably higher Young's modulus (690 MPa) than that of the PP separator (260 MPa). High Young's modulus is advantageous to remain mechanical integrity and avoid the rupture of the separator when it encounters accident crash[29].

Thermal analysis and flame retardancy. Thermal stability property of separators was another vital aspect about battery safety characteristic[19]. According to the DSC analysis shown in Figure 4a, the exothermic peak of polypropylene (PP) was related to the melting temperature of the material. The melting temperature of PP was 165°C, whereas the FCCN separator possessed superior thermal stability up to 300°C, which agreed well with the reported value in previous literature[41]. This implied that FCCN separator possessed better thermal stability than PP separator. This excellent thermal stability of FCCN separator might originate from the thermal resistance of cellulose. Therefore, FCCN separator has great potential in cells operating at an elevated temperature.

Table 1 | Physical and electrochemical parameters of PP separator and FCCN separator

Sample	Thickness (μm)	Porosity (%)	Gurley value (s/100 cc)	Uptake (%)	Ionic conductivity (mS cm^{-1})	Tortuosity
PP separator	25	55	235	125	0.65	3.1
FCCN separator	40	70	45	270	2	2

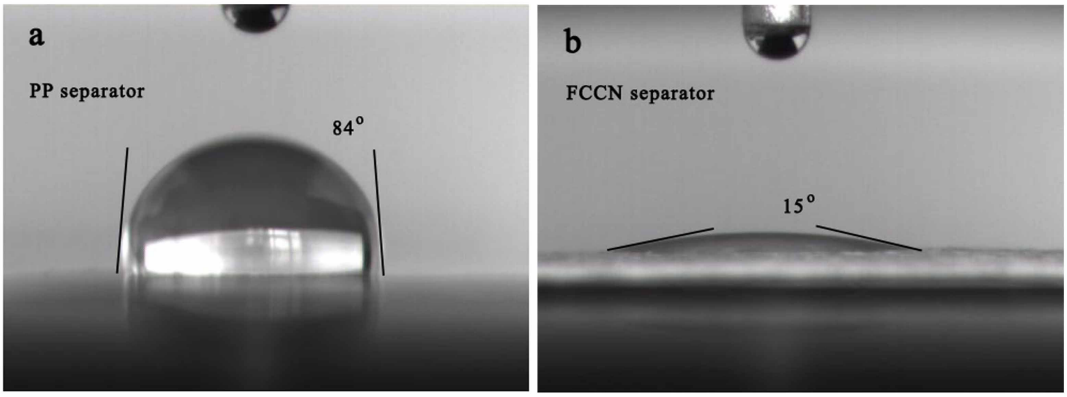

Figure 3 | Contact angle images between the separators and liquid electrolyte.

Thermal shrinkage of the separator was another essential factor to evaluate safety characteristics and battery performance of the lithium ion battery[42,43]. As shown in Figure 4b, FCCN separator exhibited negligible thermal shrinkage than that of PP separator over a wider range of temperatures. A separator must be qualified to prevent the electrodes from contacting one another at elevated temperatures[5]. The inset of Figure 4b was the photograph of PP separator and FCCN separator after thermal treatment at 150°C for 0.5 h. It can be found that FCCN separator exhibited negligible dimension change, while the PP separator generated significant shrinkage (>40%) which verified FCCN separator to exhibit excellent thermal dimensional stability. Figure 4c showed contact test between hot electric iron tip and separators. Obviously, the hole-area of PP separator propagated after hot soldering iron tip contacting test, which was detrimental to

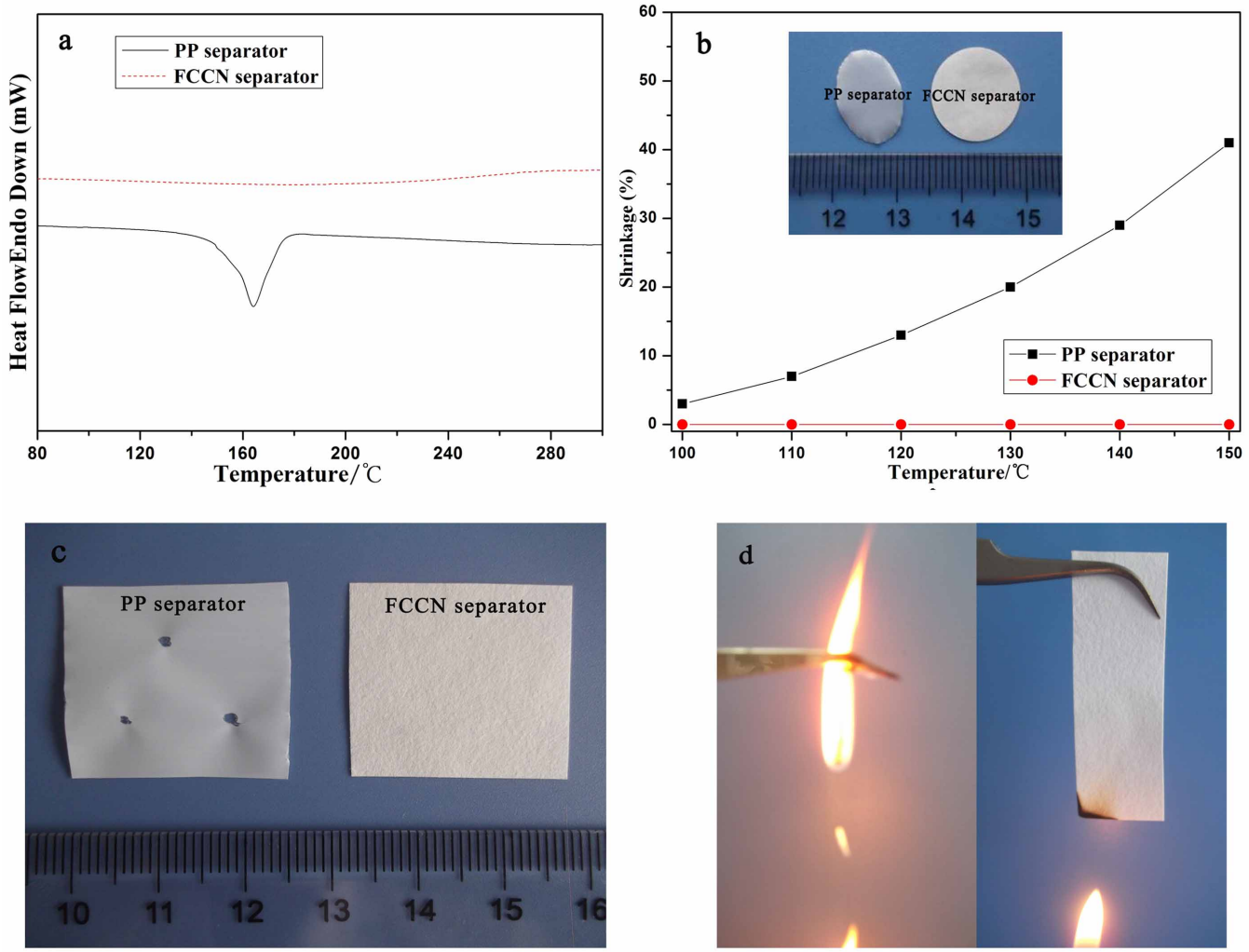

Figure 4 | (a) DSC curves of PP separator and FCCN separator, (b) Thermal shrinkage rate of PP separator and FCCN separator over a temperature range from 100°C to 150°C, and the inset is the photograph of PP separator and FCCN separator after thermal treatment at 150°C for 0.5 h, (c) Contact test between hot electric iron tip and separators, (d) Combustion behavior of PP separator and FCCN separator.

ensure safety of battery. While FCCN separator was extremely safe and had no hole. This superior thermal tolerance could effectively prevent internal electrical short circuit at elevated temperatures when the battery was operated at high charged/discharged rates[30]. Thus, FCCN separator was an advanced separator for application in LIB with requested thermal safety.

Table 2 listed limiting oxygen index (LOI) and heat release of PP separator and FCCN separator. LOI, which corresponds to the percentage of oxygen in an oxygen-nitrogen atmosphere, is used to assess flame retardancy of polymeric materials[44]. The higher the value of LOI is, the better the flame retardancy is. As Table 2 indicated, the LOI value of FCCN separator was 40%, which was much higher than that of PP separator (18%). In addition, combustion behavior of PP separator and FCCN separator was displayed in Figure 4d. PP separator ignited and burned more quickly, while FCCN separator hardly ignited. It was deduced that inflame retarding property of FCCN separator was superior to that of PP separator. Automatic oxygen bomb calorimeter was used to assess heat release value quantitatively. It was worth noting that the heat release of FCCN separator (9662 J/g) was much lower than that of PP separator (45326 J/g). The superior inflame retarding property and lower heat release of FCCN separator could significantly improve the safety characteristics of LIB.

Electrochemical characterizations. The separator must be chemically stable against the electrolyte, especially under the strongly oxidative environments[45,46]. So it is important to investigate the electrochemical stability of the electrolytes within the operation voltage of the battery system for practical battery applications. Figure S3 depicted linear sweep voltammograms for PP separator and FCCN separator. Obviously, the electrochemical working window of the electrolyte soaked PP separator was about 4.7 V *vs.* Li^+/Li, which was in good agreement with the previously reported studies[47], while that of FCCN separator was up to 4.9 V *vs.* Li^+/Li. This result indicated that FCCN separator possessed good compatibility with carbonate electrolyte when compared to that of PP separator. It is obvious that such FCCN separator is very promising for applications in high-power LIB.

Ionic conductivity is considered as a key factor of electrolyte because relatively high value can ensure better rate capability of the battery[47,48]. Figure S4 showed the Nyquist plots of liquid electrolyte-soaked PP separator and FCCN separator. The intercept of the semicircle with the real axis was the electrolyte bulk resistance (R_b). The ionic conductivity was then calculated from the R_b values by employing the formula: $\sigma = L/R_bA$, where L was the thickness of the separator sample and A was the contact area between the separator and the electrode. It can be obtained that the ionic conductivity of FCCN separator was 2.0×10^{-3} S cm^{-1}, which was much higher than that of PP separator (0.65×10^{-3} S cm^{-1}). The interconnected porous structure and polar chemical composition of FCCN separator was benificial to higher ionic conductivity[49].

The interfacial compatibility of lithium metal with separator was another factor to affect battery performance[50]. Figure S5 depicted the interfacial compatibility of the liquid electrolyte-soaked separators with a lithium metal anode, which was characterized by the electrochemical impedance spectroscopy. It could be observed that the interfacial resistance was 170 Ω for FCCN separator and 350 Ω for PP separator, respectively. Obviously, the interfacial property between anode and separator can be significantly improved in the case of FCCN separator, which indicated that FCCN separator could endow better interfacial characteristics for lithium battery separator[21].

Table 2 | LOI and heat release of PP separator and FCCN separator

Samples	PP separator	FCCN separator
LOI (%)	18	40
Heat Release (J/g)	45326	9662

Discussion

The practical application of FCCN separator for LIB was explored in terms of cell performance, which included rate capability and cycle performance. Figure 5a displayed rate capability plots of the $LiCoO_2$/graphite cells from 2.75 to 4.20 V at different rates (0.2 C, 0.5 C, 1.0 C, 2.0 C, 4.0 C and 8.0 C). It can be observed from Figure 5a that the cell at 0.2 C achieved the highest specific capacity, 129 mAh g^{-1} for FCCN separator and 128 mAh g^{-1} for PP separator. In addition, the discharge capacities of the cell using FCCN separator decreased with increasing discharge rates, but it still kept relatively high capacity as a whole. In the case of the cells with FCCN separator, the capacity kept 107 mAh g^{-1} at 4 C and 83 mAh g^{-1} at 8 C rate, respectively. However, the capacity of the cells employing PP separator decreased rapidly to 86 mAh g^{-1} at 4 C and 47 mAh g^{-1} at 8 C, respectively. It was reasonable to deduce that the FCCN separator exhibited much better rate capability when compared to that of PP separators. Superior rate performance was ascribed to the higher ionic conductivity and lower interfacial resistance of FCCN separator[51–53]. In fact, for the high-energy commercial LIB, 8 C is enough for high power. Hence, FCCN separator is highly suitable separator for high energy lithium ion battery.

Cycling stability was also an important parameter for rating lithium ion battery[47]. Figure 5b presented the cycling stability of the $LiCoO_2$/graphite cells using PP separator and FCCN separator at 0.5 C/0.5 C up to 200 cycles. As shown in Figure 5b, the cells with FCCN separator showed stable cycling performance and higher capacity retention ratio than that of PP separator after 200 cycles. The obtained capacity retention after 200 cycles for the cells was 75% for FCCN separator and 61% for PP separator, respectively. The better cycling stability of the cells using FCCN separator could be attributed to its better electrolyte retention and more compatible interface than that of PP separator[54].

To investigate the variation of cell impedances during cycling, AC impedance measurement was carried out for $LiCoO_2$/graphite cells assembled with PP separator and FCCN separator after the first cycle and after the 200 cycles test. It is well known that the semicircle at high frequency zone represents the charge-transfer resistance accompanied with migration of lithium ion between the electrode and electrolyte interface. The straight slopping line corresponds to the diffusion of lithium ion in the active material of electrode[55]. It can be seen from Figure 5c that the charge-transfer resistance of the cell using FCCN separator after the first cycle was 20 Ω, which was very close to that of PP separator. It was quite obvious to observe from Figure 5d that the charge-transfer resistance of the cell using FCCN separator after the 200 cycles test was 42 Ω, whereas that of the PP displayed 130 Ω. The better charge-transfer behavior of FCCN separator was directly related to excellent interface stability and improved electrolyte retention in FCCN separator[28]. Better rate capability and cycle performance of the cell with FCCN separator would be attributed to the limited cell impedance increase during long term cycling and improved electrolyte retention of FCCN separator.

For practical battery applications, it is important to investigate the cycle performance not only at room temperature, but also at elevated temperature[56]. Herein, we selected $LiFePO_4$ as the preferred cathode material owing to its better performance at elevated temperature[57]. Figure 6 depicted cycle performance and charge/discharge curves of $LiFePO_4$/Li cells using PP separator and FCCN separator at 120°C. As revealed in Figure 6a, the $LiFePO_4$/Li cell using FCCN separator exhibited much better cycling performance than PP separator. Moreover, it can be easily observed in Figure 6b that the $LiFePO_4$/Li cell using FCCN separator can sustain stable charge/discharge curves, in contrast, PP separator could not even be stably charged and discharged at 120°C. The main reason was associated with sig-

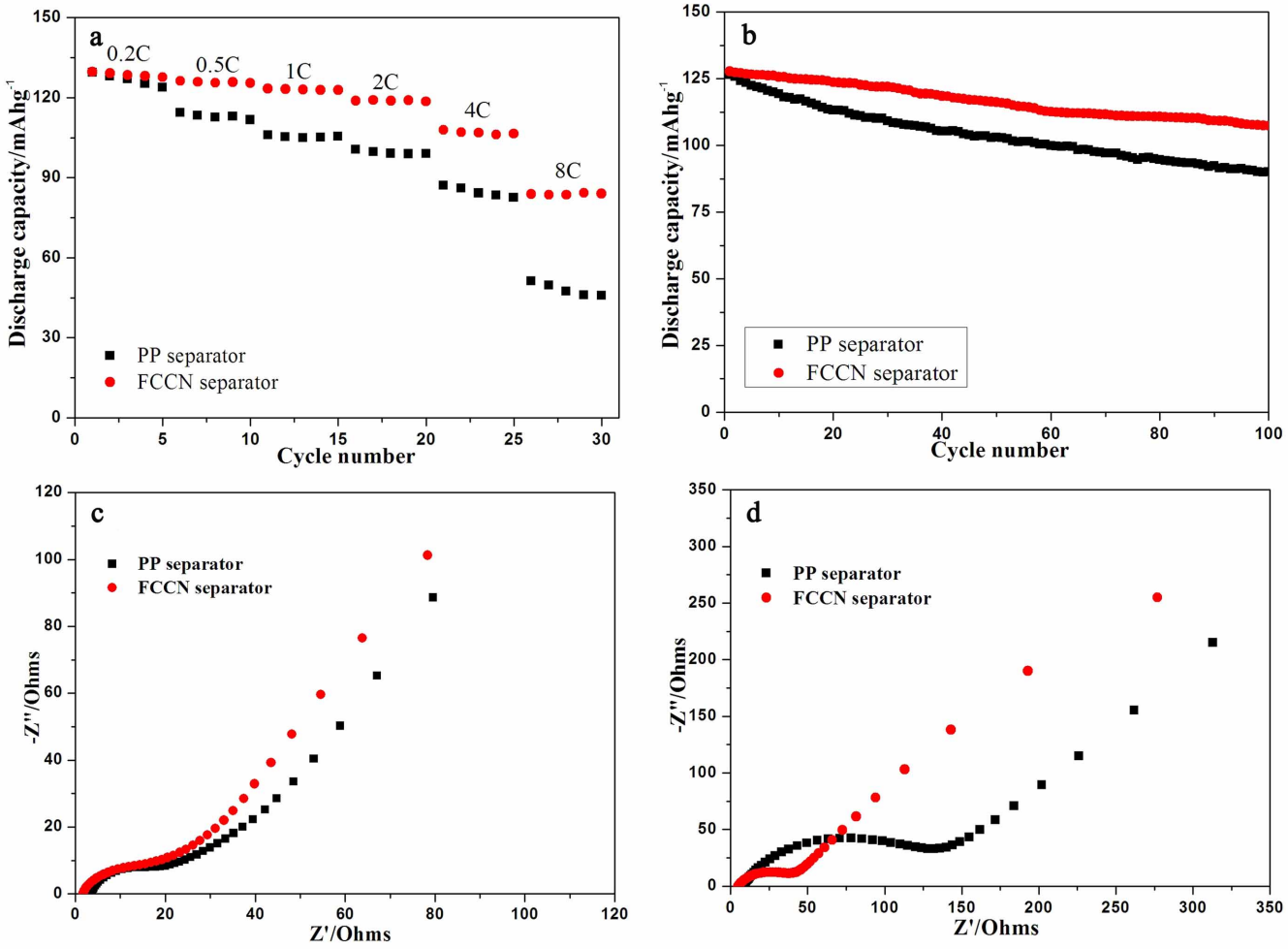

Figure 5 | (a) Rate capability and (b) cycling stability of the $LiCoO_2$/graphite cells using PP separator and FCCN separator. Nyquist plots for the $LiCoO_2$/graphite cells using PP separator and FCCN separator measured (c) after the first cycle and (d) after the 200 cycles test.

nificant thermal shrinkage of PP separator at the elevated temperature, which caused internal short-circuits in the cell. These results demonstrated that FCCN separator possessed better thermal stability and would enhance safety characteristic of LIB. From the above mentioned discussion, it is abundantly clear that FCCN nonwoven is very promising for high-power LIB separator.

In conclusion, a cellulose-based composite separator with good electrolyte wettability, high ionic conductivity, excellent flame retardancy and superior thermal resistance was developed for improving the safety characteristics of LIB. It was demonstrated that the $LiCoO_2$/graphite cell using FCCN separator displayed better rate capability and enhanced capacity retention when compared to those

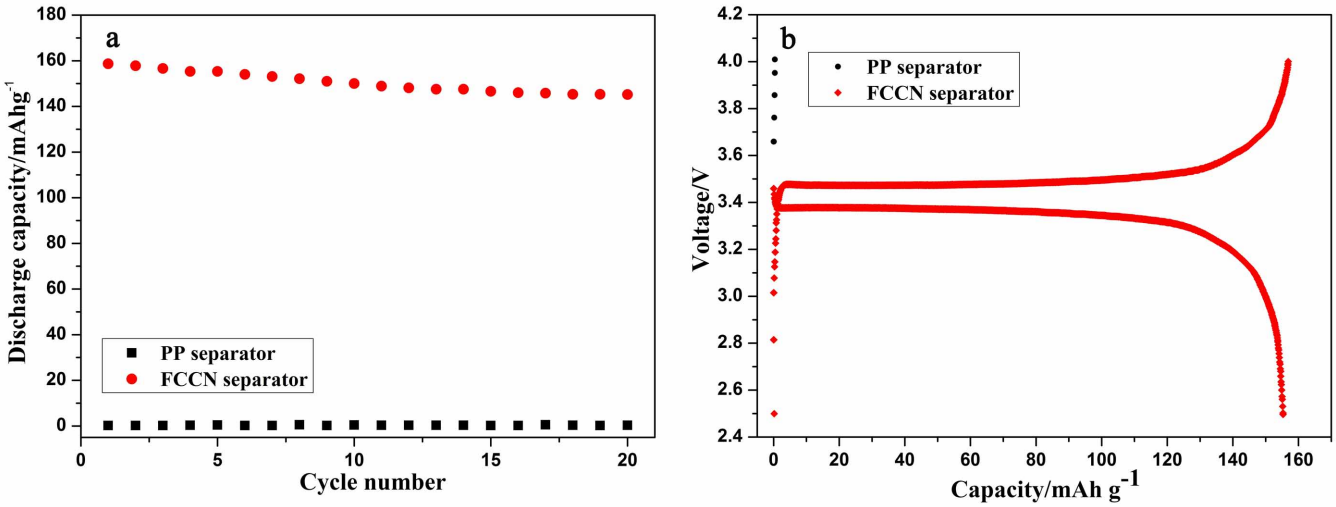

Figure 6 | (a) Cycle performance and (b) charge/discharge curves for $LiFePO_4$/Li cells using PP separator and FCCN separator at 120°C.

of PP separator. In addition, FCCN separator based lithium iron phosphate ($LiFePO_4$)/lithium (Li) cell exhibited stable charge-discharge profiles and satisfactory cycling stability even at an elevated temperature of 120°C. Those advantages endow it a promising separator for LIB that powers consumer electronics and hybrid electric vehicles. All these results suggest that such FCCN separator is also very attractive in other electrochemical devices (such as sodium ion battery, lithium-sulfur battery and super capacitor).

Methods

Sample collection. PP separator (Celgard 2500) used as comparative analysis was purchased from Celgard Company (USA). Cellulose pulp was supplied by Shandong Yinying Chemical Co., Ltd (China). Nitrogen- Phosphorus complex flame retardant (FR) was purchased from Qingdao Haihua flame-retardant materials Co., Ltd. (Shandong, China). Sodium alginate (SA) was provided by the Qingdao Mingyue Company (Shandong, China). Silica nanoparticle (30 nm) was supplied by Guangcheng Chemistry Reagents Ltd. (Tianjin, China). Other chemical reagents were all purchased commercially and used without further purification. Valley beating machine (ZDJ100) was offered by Shandong Yinying Chemical Co., Ltd (China). Papermaking machine was purchased from Estanit GbmH Co., Ltd. (German).

Samples characterization. The morphology of the separators was observed using a field emission scanning electron microscope (Hitachi S-4800 at 3 kV). The thickness of each separator was measured using a micrometer. The air permeability was obtained using a Gurley-type densometer (4110N, Gurley) by measuring the time of 100 cc air to pass through the separator. The porosity was measured by immersing the separator into n-butanol for 2 h and calculating with the following equation: Eq. (1): $P = [(m_b/\rho_b)/(m_b/\rho_b + m_a/\rho_a)] \times 100\%$, where m_a and m_b were the mass of the separator and n-butanol, ρ_a and ρ_b were the density of separator material and n-butanol, respectively. The liquid electrolyte uptake was determined by following Eq. (2): $EU = [(W - W_o)/W_o] \times 100\%$, where W_o and W indicated the separator weight before and after liquid electrolyte absorption, respectively. The extra solution (n-butanol or electrolyte) at the surface of the separator was absorbed with a filter paper before measuring the weight. Contact angle measurement was performed using a JC2000C Contact Angle Meter. Contact angle of 5 μL electrolyte droplet was measured using a JC2000C Contact Angle Meter. Tortuosity of the membranes was calculated by using the relationship: $\tau = \left(\frac{\sigma_0}{\sigma} \times P\right)^{1/2}$, where σ_0 and σ are the conductivity of the neat liquid electrolyte and electrolyte-soaked membrane, respectively, and P is the porosity of membrane. The stress-strain curves of the separators were tested using an Instron-3300 universal tensile tester (USA) at a speed of 10 mm min^{-1} using samples with 1 cm in width and 8 cm in length. Young's modulus (E) can be calculated with the following equation: Eq. (3): $E = \sigma/\varepsilon$, where σ and ε stress and strain of the separator. Differential scanning calorimeter (Diamond DSC, PerkinElmer) was used to evaluate the thermal properties of the separators. Samples were scanned from 50°C to 300°C at a heating rate of 10°C/min under a N_2 atmosphere. To evaluate its thermal shrinkage behavior, the separator was placed in an oven and heated at 150°C for 0.5 h. Thermal shrinkage ratio (TSR) was calculated according to Eq. (4): $TSR\ (\%) = (S_o - S/S_o) \times 100\%$. Here, S_o and S represent the area of the separator before and after thermal treatment at a series of temperature for 0.5 h, respectively. Contact test between hot electric iron tip and separator was performed as follows: Soldering iron tip was first heated to 400°C and contacted to separator gently for 1 second, then recorded the changes of surface morphology of separator. Limiting oxygen index (LOI) measurement was undertaken using JF-3 type oxygen index tester (China). Heat release value was determined by automatic oxygen bomb calorimeter (IKA C200, German).

Electrochemical evaluation. The separators for the electrochemical stability measurement were sandwiched between lithium metal and stainless steel electrode in a test cell. And then the electrochemical stability was measured by using a liner sweep voltammetry at a scan rate of 1.0 mV s^{-1} from 2.5 V to 6 V. The ionic conductivity and cell resistance were evaluated via AC impedance analyses (Zennium) over a frequency range from 1 Hz to 10^6 Hz and under an AC voltage of 10 mV. The ionic conductivity was then calculated by using formula: $\sigma = L/R_bA$, where L was the thickness of the separator and A was the contact area between the separator and the stainless steel electrode, R_b was the bulk resistance. The full coin cells (2032-type) with $LiCoO_2$ cathode, graphite anode and separator soaked with liquid electrolyte were assembled in a argon-filled glove box. The anode had a composition of 93 wt% graphite, 2 wt% carbon black, 1.5 wt% CMC and 3.5 wt% SBR as a polymeric binder. The cathode was composed of 90 wt% $LiCoO_2$, 5 wt% carbon black, and 5 wt% PVdF. The electrolyte was $LiPF_6$ (1 M) with ethylene carbonate (EC)/dimethyl carbonate (DMC) (1 : 1 v/v). The rate capability and cycling stability were performed using a LAND battery testing system. The charge/discharge current densities were varied from 0.2 C (20 mA g^{-1}) to 8.0 C (800 mA g^{-1}) for rate capability under a voltage range between 2.75 V and 4.2 V. The cells were cycled at a fixed charge/discharge current density of 0.5 C (50 mA g^{-1})/0.5 C (50 mA g^{-1}). A coil cell (2032-type) was assembled by sandwiching a separator between a lithium metal foil anode and a $LiFePO_4$ cathode and then filling liquid electrolyte. The $LiFePO_4$ cathode was composed of 90 wt% $LiFePO_4$, 10 wt% carbon black, and 5 wt% PVdF. The electrolyte was lithium bis(oxalate)borate LiBOB (1 M) with propylene carbonate (PC). Cycling stability of the cells was characterized using a LAND battery testing system at an elevated temperature of 120°C. The cells were cycled at a fixed charge/discharge current density of 0.5 C/0.5 C under a voltage range between 2.5 V and 4.0 V.

1. Arora, P. & Zhang, Z. M. Battery separators. *Chem. Rev.* **104**, 4419–4462 (2004).
2. Koo, B. *et al.* A highly cross-linked polymeric binder for high-performance silicon negative electrodes in lithium ion batteries. *Angew. Chem. Int. Ed.* **51**, 8762–8767 (2012).
3. Li, H., Wang, Z., Chen, L. & Huang, X. Research on advanced materials for Li-ion batteries. *Adv. Mater.* **21**, 4593–4607 (2009).
4. Cui, G. L. *et al.* A germanium–carbon nanocomposite material for lithium batteries. *Adv. Mater.* **20**, 3079–3083 (2008).
5. Zhou, X. H. *et al.* A core-shell structured polysulfonamide-based composite nonwoven towards high power lithium ion battery separator. *J. Electrochem. Soc.* **160**, A1341–A1347 (2013).
6. Cui, G. L. *et al.* A novel germanium/carbon nanotubes nanocomposite for lithium storage material. *Electrochim. Acta* **55**, 985–988 (2010).
7. Palacin, M. R. Recent advances in rechargeable battery materials: a chemist's perspective. *Chem. Soc. Rev.* **38**, 2565–2575 (2009).
8. Scrosati, B. & Garche, J. Lithium batteries: Status, prospects and future. *J. Power Sources* **195**, 2419–2430 (2010).
9. Hu, Y. S. *et al.* Superior storage performance of a Si@SiOx/C nanocomposite as anode material for lithium-ion batteries. *Angew. Chem. Int. Ed.* **47**, 1645–1649 (2008).
10. Zhao, L., Hu, Y. S., Li, H., Wang, Z. X. & Chen, L. Q. Porous $Li_4Ti_5O_{12}$ coated with N-Doped carbon from ionic liquids for Li-ion batteries. *Adv. Mater.* **23**, 1385–1388 (2011).
11. Maier, J. Thermodynamics of electrochemical lithium storage. *Angew. Chem. Int. Ed.* **52**, 4998–5026 (2013).
12. Suo, L. M., Hu, Y. S., Li, H., Armand, M. & Chen, L. Q. A new class of solvent-in-salt electrolyte for high-energy rechargeable metallic lithium batteries. *Nat. Commun.* **4**, 1481 (2013).
13. Ding, N. *et al.* Improvement of cyclability of Si as anode for Li-ion batteries. *J. Power Sources* **192**, 644–651 (2009).
14. Li, H., Wang, Z. X., Chen, L. Q. & Huang, X. J. Research on advanced materials for Li-ion batteries. *Adv. Mater.* **21**, 4593–4607 (2009).
15. Huang, X. S. Separator technologies for lithium-ion batteries. *J. Solid State Electrochem.* **15**, 649–662 (2011).
16. Zhang, J. J. *et al.* A highly safe and inflame retarding aramid lithium ion battery separator by a papermaking process. *Solid State Ionics* **245–246**, 49–55 (2013).
17. Kim, M., Shon, J. Y., Nho, Y. C., Lee, T. W. & Park, J. H. Positive Effects of E-Beam Irradiation in Inorganic Particle Based Separators for Lithium-Ion Battery. *J. Electrochem. Soc.* **157**, A31–A34 (2010).
18. Ryou, M. H., Lee, Y. M., Park, J. K. & Choi, J. W. Mussel-inspired polydopamine-treated polyethylene separators for high-power Li-Ion batteries. *Adv. Mater.* **23**, 3066–3070 (2011).
19. Zhang, S. S. A review on the separators of liquid electrolyte Li-ion batteries. *J. Power Sources* **164**, 351–364 (2007).
20. Lee, H., Alcoutlabi, M., Watson, J. V. & Zhang, X. W. Electrospun nanofiber-coated separator membranes for lithium-ion rechargeable batteries. *J. Appl. Polym. Sci.* **129**, 1939–1951 (2013).
21. Jeong, H. S., Kim, J. H. & Lee, S. Y. A novel poly(vinylidene fluoride-hexafluoropropylene)/poly(ethylene terephthalate) composite nonwoven separator with phase inversion-controlled microporous structure for a lithium-ion battery. *J. Mater. Chem.* **20**, 9180–9186 (2010).
22. Etacheri, V., Marom, R., Elazari, R., Salitra, G. & Aurbach, D. Challenges in the development of advanced Li-ion batteries: a review. *Energy Environ. Sci.* **4**, 3243–3262 (2011).
23. Zhou, L. *et al.* Facile in-situ synthesis of manganese dioxide nanosheets on cellulose fibers and their application in oxidative decomposition of formaldehyde. *J. Phys. Chem. C* **115**, 16873–16878 (2011).
24. Wang, Z. H., Chien, W. C., Yue, T. W. & Tang, S. C. Application of heparinized cellulose affinity membranes in recombinant adeno-associated virus serotype 2 binding and delivery. *J. Membrane Sci.* **310**, 141–148 (2008).
25. Jackson, E. L. & Hudson, C. S. Application of the cleavage type of oxidation by periodic acid to starch and cellulose. *J. Am. Chem. Soc.* **59**, 2049–2050 (1937).
26. Cherian, B. M. *et al.* Cellulose nanocomposites with nanofibres isolated from pineapple leaf fibers for medical applications. *Carbohydr. Polym.* **86**, 1790–1798 (2011).
27. Kuribayashi, I. Characterization of composite cellulosic separators for rechargeable lithium-ion batteries. *J. Power Sources* **63**, 87–91 (1996).
28. Chun, S. J. *et al.* Eco-friendly cellulose nanofiber paper-derived separator membranes featuring tunable nanoporous network channels for lithium-ion batteries. *J. Mater. Chem.* **22**, 16618–16626 (2012).
29. Zhang, J. J. *et al.* Renewable and superior thermal-resistant cellulose-based composite nonwoven as lithium-ion battery separator. *ACS Appl. Mater. Interfaces* **5**, 128–134 (2013).

30. Kim, J. H. *et al.* Colloidal silica nanoparticle-assisted structural control of cellulose nanofiber paper separators for lithium-ion batteries. *J. Power Sources* **242**, 533–540 (2013).
31. Garvey, S. J., Anand, S. C., Rowe, T., Horrocks, A. R. & Walker, D. G. The flammability of hybrid viscose blends. *Polym. Degrad. Stab.* **54**, 413–416 (1996).
32. Heidari, S. & Kallonen, R. Hybrid fibres in fire protection. *Fire Mater.* **17**, 21–24 (1993).
33. Ding, J., Kong, Y., Li, P. & Yang, J. R. Polyimide/poly(ethylene terephthalate) composite membrane by electrospinning for nonwoven separator for lithium-ion battery. *J. Electrochem. Soc.* **159**, A1474–A1480 (2012).
34. Hao, J. L. *et al.* A novel polyethylene terephthalate nonwoven separator based on electrospinning technique for lithium ion battery. *J. Membrane Sci.* **428**, 11–16 (2013).
35. Prasanna, K. & Lee, C. W. Physical, thermal, and electrochemical characterization of stretched polyethylene separators for application in lithium-ion batteries. *J Solid State Electr.* **17**, 1377–1382 (2013).
36. Qi, W. *et al.* Electrochemical performances and thermal properties of electrospun Poly(phthalazinone ether sulfone ketone) membrane for lithium-ion battery. *Mater. Lett.* **66**, 239–241 (2012).
37. Wang, Y., Zhan, H. Y., Hu, J., Liang, Y. & Zeng, S. S. Wet-laid non-woven fabric for separator of lithium-ion battery. *J. Power Sources* **189**, 616–619 (2009).
38. Ryou, M. H., Lee, Y. M., Park, J. K. & Choi, J. W. Mussel-Inspired Polydopamine-Treated Polyethylene Separators for High-Power Li-Ion Batteries. *Adv. Mater.* **23**, 3066–3070 (2011).
39. Liu, K. S., Yao, X. & Jiang, L. Recent developments in bio-inspired special wettability. *Chem. Soc. Rev.* **39**, 3240–3255 (2010).
40. Liu, Z. H. *et al.* A Core@sheath nanofibrous separator for lithium ion batteries obtained by coaxial electrospinning. *Macromol. Mater. Eng.* **298**, 806–813 (2012).
41. Liu, H. Q. & Hsieh, Y. L. Ultrafine fibrous cellulose membranes from electrospinning of cellulose acetate. *J. Polym. Sci. Phys.* **40**, 2119–2129 (2002).
42. Xiong, M. *et al.* Expanded polytetrafluoroethylene reinforced polyvinylidenefluoride–hexafluoropropylene separator with high thermal stability for lithium-ion batteries. *J. Power Sources* **241**, 203–211 (2013).
43. Wu, N., Cao, Q., Wang, X. Y. & Chen, Q. Q. Study of a novel porous gel polymer electrolyte based on TPU/PVdF by electrospinning technique. *Solid State Ionics* **203**, 42–46 (2011).
44. Zhang, J. J., Ji, Q., Wang, F. J., Tan, L. W. & Xia, Y. Z. Effects of divalent metal ions on the flame retardancy and pyrolysis products of alginate fibres. *Polym. Degrad. Stabil.* **97**, 1034– (2012).
45. Cai, Z., Liu, Y., Liu, S., Li, L. & Zhang, Y. High performance of lithium-ion polymer battery based on non-aqueous lithiated perfluorinated sulfonic ion-exchange membranes. *Energy Environ. Sci.* **5**, 5690–5693 (2012).
46. Sirisopanaporn, C., Fernicola, A. & Scrosati, B. New, ionic liquid-based membranes for lithium battery application. *J. Power Sources* **186**, 490–495 (2009).
47. Ulaganathan, M., Nithya, R., Rajendran, S. & Raghu, S. Li-ion conduction on nanofiller incorporated PVdF-co-HFP based composite polymer blend electrolytes for flexible battery applications. *Solid State Ionics* **218**, 7–12 (2012).
48. Croce, F., Focarete, M. L., Hassoun, J., Meschini, I. & Scrosati, B. A safe, high-rate and high-energy polymer lithium-ion battery based on gelled membranes prepared by electrospinning. *Energy Environ. Sci.* **4**, 921–927 (2011).
49. Zhang, L. C., Sun, X., Hu, Z., Yuan, C. C. & Chen, C. H. Rice paper as a separator membrane in lithium-ion batteries. *J. Power Sources* **204**, 149–154 (2012).
50. Xu, K. Nonaqueous Liquid Electrolytes for Lithium-Based Rechargeable Batteries. *Chem. Rev.* **104**, 4303–4417 (2004).
51. Jabbour, L. *et al.* Aqueous processing of cellulose based paper-anodes for flexible Li-ion batteries. *J. Mater. Chem.* **22**, 3227–3233 (2012).
52. Prasanth, R., Aravindan, V. & Srinivasan, M. Novel polymer electrolyte based on cob-web electrospun multi component polymer blend of polyacrylonitrile/poly(methyl methacrylate)/polystyrene for lithium ion batteries-Preparation and electrochemical characterization. *J. Power Sources* **202**, 299–307 (2012).
53. Kim, J. Y. & Lim, D. Y. Surface-Modified Membrane as A Separator for Lithium-Ion Polymer Battery. *Energies* **3**, 866–885 (2010).
54. Jiang, W. *et al.* A high temperature operating nanofibrous polyimide separator in Li-ion battery. *Solid State Ionics* **232**, 44–48 (2013).
55. Zhang, K. J. *et al.* Synthesis of nitrogen-doped MnO/graphene nanosheets hybrid material for lithium ion batteries. *ACS Appl. Mater. Inter.* **4**, 658–664 (2012).
56. Wen, J. W., Yu, Y. & Chen, C. H. A review on lithium-ion batteries safety issues: existing problems and possible solutions. *Mater Express* **2**, 197–212 (2012).
57. Huang, Y. H., Dass, R. I., Xing, Z. L. & Goodenough, J. B. Double perovskites as anode materials for solid-oxide fuel cells. *Science* **312**, 254–257 (2006).

Acknowledgments

This work was financially supported by the National Program on Key Basic Research Project of China (973 Program) (No. MOST2011CB935700), the Instrument Developing Project of the Chinese Academy of Sciences (No. YZ201137) and the National High Technology Research and Development Program of China (863 Program, No. 2013AA050905).

Author contributions

J.J.Z., G.L.C. and L.Q.C. devised the original concept, designed the experiments and discussed the interpretation of results. J.J.Z. and L.P.Y. co-wrote the paper. Q.S.K., Z.H.L. and X.H.Z. fabricated the separator. C.J.Z., Q.X., B.Z. and G.L.D. optimized the polymer separator. B.S.Q., Y.L.D., Q.F.W. and J.H.Y. performed the electrochemical experiments. All authors discussed the results and participated in manuscript revision.

Additional information

Supplementary information accompanies this paper at http://www.nature.com/scientificreports

Competing financial interests: The authors declare no competing financial interests.

How to cite this article: Zhang, J.J. *et al.* Sustainable, heat-resistant and flame-retardant cellulose-based composite separator for high-performance lithium ion battery. *Sci. Rep.* **4**, 3935; DOI:10.1038/srep03935 (2014).